

Supplementary for Oxymatrine Modulation of TLR3 Signaling: A Dual-Action Mechanism for H9N2 Avian Influenza Virus Defense and Immune Regulation

Yan Zhi †, Xinping Zhao †, Zhenyi Liu, Guoyu Shen, Taiming Zhang, Tao Zhang and Ge Hu *

College of Animal Science and Technology, Beijing University of Agriculture, Beijing 102206, China;
bjzhiyan@sina.com (Y.Z.); 202130311012@bua.edu.cn (X.Z.); liuzylenn@163.com (Z.L.); zytgzyyx0723@163.com (G.S.);
202330311012@bua.edu.cn (T.Z.); zhangtao8008@126.com (T.Z.)

* Correspondence: bnhuge@126.com; Tel.: +86 13693501841

† These authors contributed equally to this work.

This file includes:

Tables S1–S3

Figures S1–S5

Content list

Supplementary Tables

Table S1 -----	1
Table S2 -----	2
Table S3 -----	3

Supplementary Figures

Figure S1 -----	4
Figure S2 -----	5
Figure S3 -----	6
Figure S4 -----	7
Figure S5 -----	8

Table S1. siRNA sequences

Group	Target Sequence	siRNA Sequence
TLR3 RNAi	si-TLR3-1-ss	GGUGAGCAGUUCGAAUACATT
	si-TLR3-1-as	UGUAUUCGAACUGCUCACCTT
	si-TLR3-2-ss	GUUCAAGAACUUAUUCGAATT
	si-TLR3-2-as	UUCGAAUAAGUUCUUGAACTT
	si-TLR3-3-ss	CAUGGACGAUAAUACUAUATT
	si-TLR3-3-as	UAUAGUAUUAUCGUCCAUGTT
Negative Control	TLR3-negative	siRNA Negative Control

Note: The aforementioned siRNA sequences, along with the negative control sequence, were subjected to NCBI's BLAST search and showed specificity only to the rat genome, exclusively aligning with the TLR3 sequence, ensuring no off-target effects on other genes.

Table S2. Quantitative Real-time PCR Primer sequences

Genes	Primer Direction	Sequences (5'→3')
PKR	Forward primer	CCGGATCCAGAAAGTCGGTC
	Reverse primer	TTCGCCTCCTGCTTTGATCT
Mx1	Forward primer	CGGAGGATTGGTAAGCCCTCT
	Reverse primer	TATCCACAGACTCCATTGCCTG
TLR3	Forward primer	GGTCAGTTTATGAATTCCAGGAGG
	Reverse primer	GGGCAGTTTTACTTCCCCGA
NF-κB	Forward primer	ATACCACTGTCAACAGATGGCCC
	Reverse primer	TTCCATTTGTGACCAACTGAACG
IRF-3	Forward primer	GTATGCGCAGGCTGGATCA
	Reverse primer	CAGGTTGACAGGTCTGGCTT
β-actin	Forward primer	CCCGCGAGTACAACCTTCTT
	Reverse primer	CCATACCCACCATCACACCC
NAPDH	Forward primer	CCCCCATGTTTGTGATGGGT
	Reverse primer	GCACGATGCATTGCTGACAA

Table S3. Effects of different low concentrations of OMT on the survival rate of PMVECs

Time (h)	OMT Concentration ($\mu\text{g/ml}$)							
	0	2.5	5	7.5	10	12.5	15	
12	100.00	100.76	97.36	96.94	94.92	100.11	100.74	
24	100.00	99.52	97.92	96.15	94.76	94.29	98.55	
36	100.00	100.07	98.88	103.82	95.78	92.53	88.35	
48	100.00	99.29	100.50	97.85	94.77	91.27	87.93	

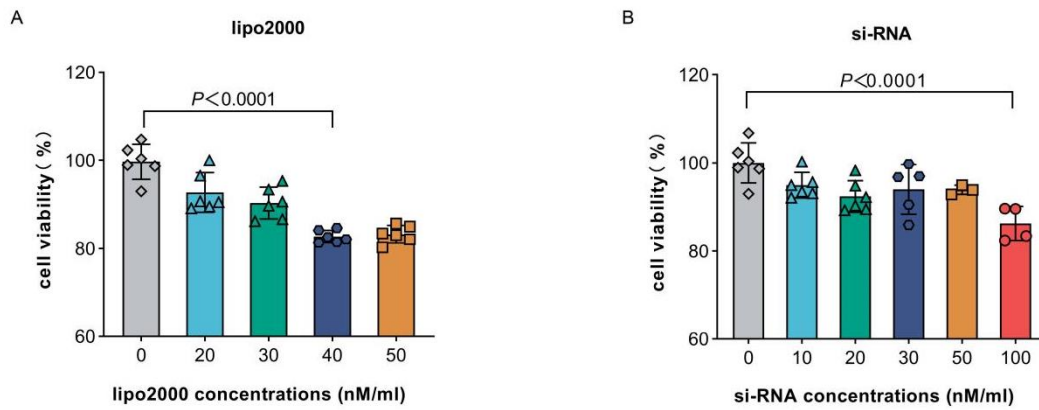


Figure S1. Safe concentration of siRNA and transfection reagent.

(A) Determination of the safe concentration for transfection reagent.

(B) Selection of the optimal concentration for siRNA.

Experiments were performed as three biologically independent experiments, and the mean \pm S.D. (n = 6) is shown. P values were determined by non-parametric one-way ANOVA.

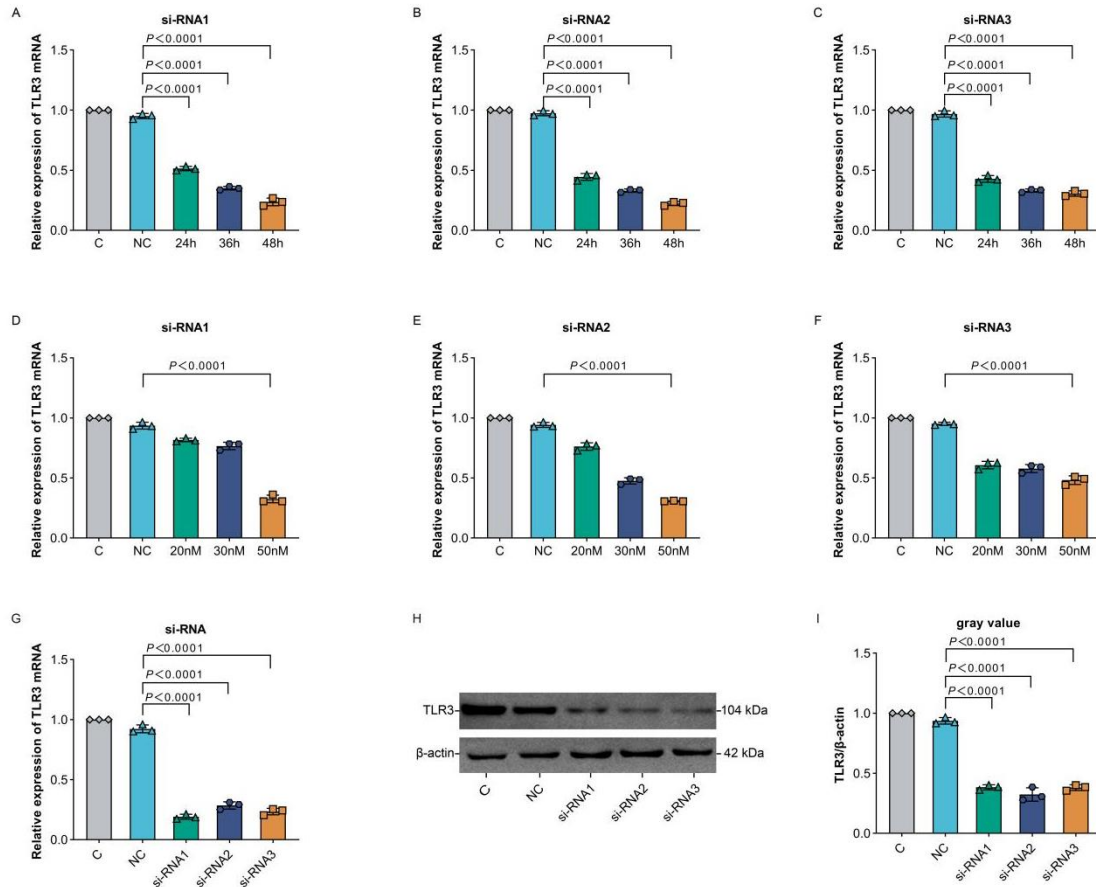


Figure S2. Evaluation of siRNA's temporal, concentration, and sequence efficacy.

(A-C) Effects of different siRNAs on the relative expression of TLR3 mRNA under different action time.

(D-F) Effect of different siRNAs on the relative expression of TLR3 mRNA.

(G-I) Effect of different siRNAs on the relative expression of TLR3 protein.

Experiments were performed as three biologically independent experiments, and the mean \pm S.D. ($n = 3$) is shown. P values were determined by non-parametric one-way ANOVA.

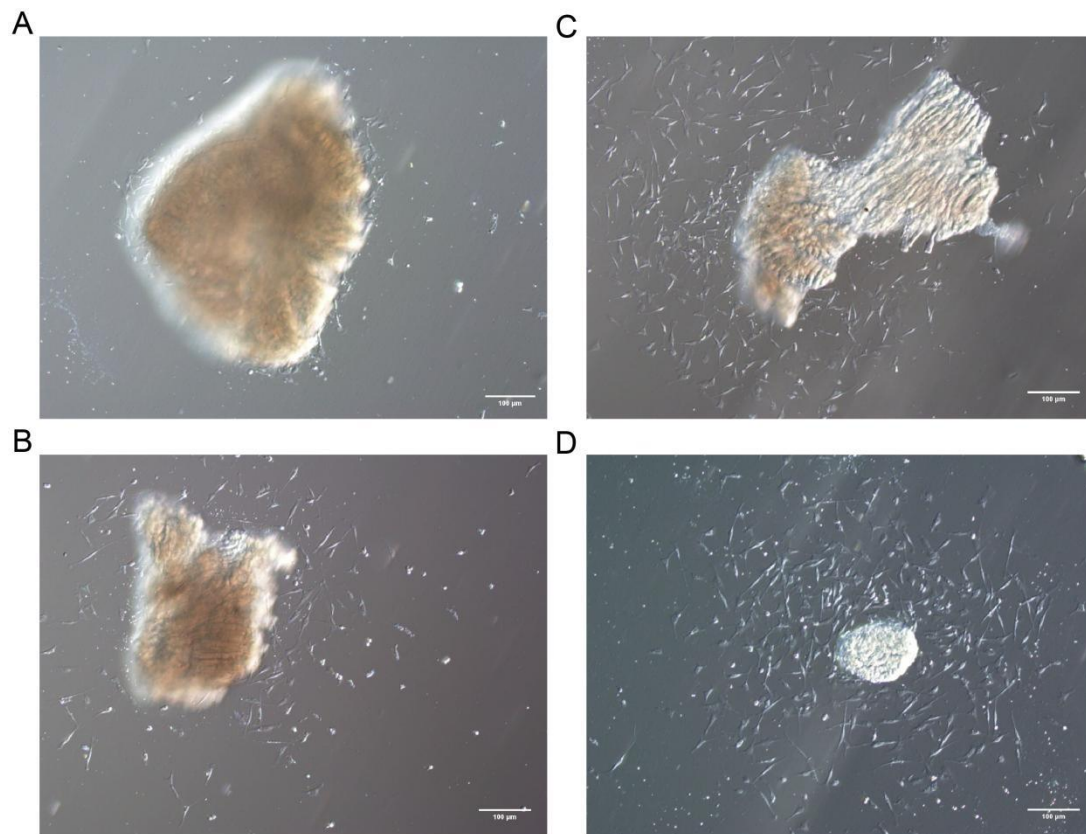


Figure S3. Monitoring of morphological changes and migration in primary isolated PMVECs over time

(A) Migration initiation from the tissue block periphery observed at around 6 hours post-culture initiation.

(B-D) Escalation of migration from the tissue block periphery over time, captured under phase-contrast microscopy at various time points. Scale bar = 100 µm

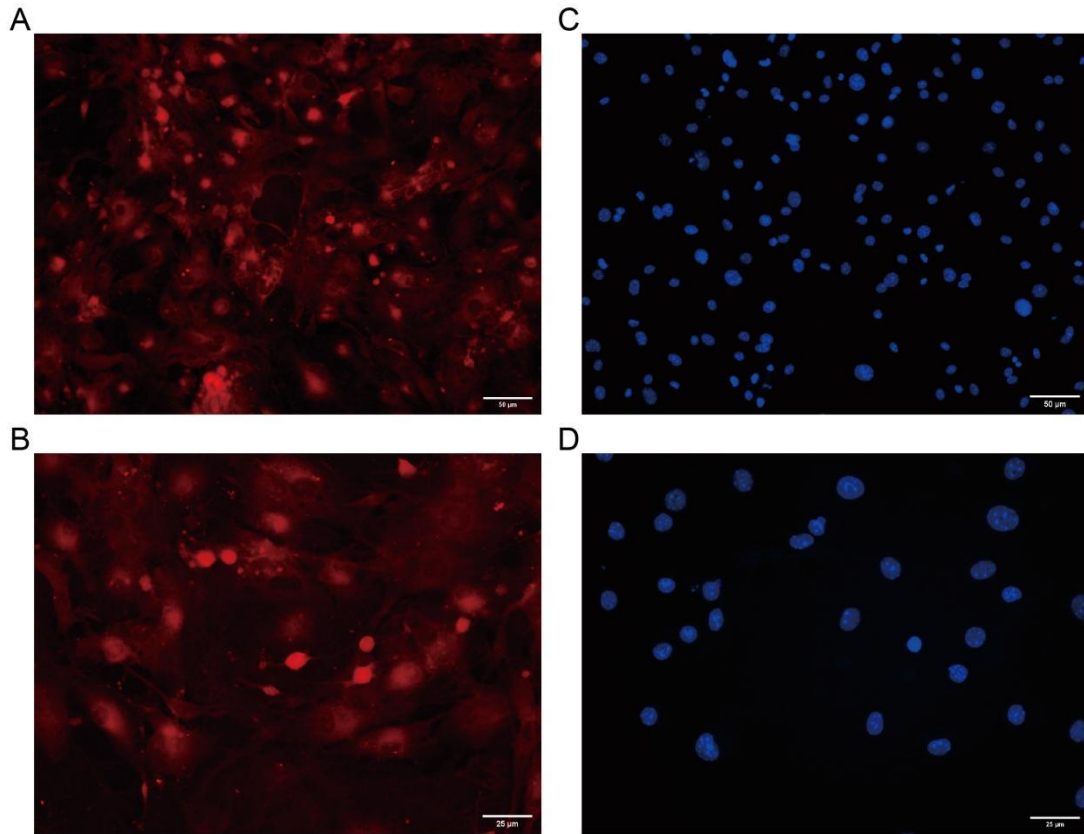


Figure S4. CD31 Expression in PMVECs Identified through Immunofluorescence Staining

(A-B) Immunofluorescence identification of CD31 antigen in PMVECs. Images at 200x (A) and 400x (B) magnification depict CD31 expression with red staining. Scale bar =50 μm and 25 μm.

(C-D) Immunofluorescence identification of CD31 antigen in PMVECs. Images at 200x (C) and 400x (D) magnification show nuclei with blue staining by DAPI. Scale bar =50 μm and 25 μm.

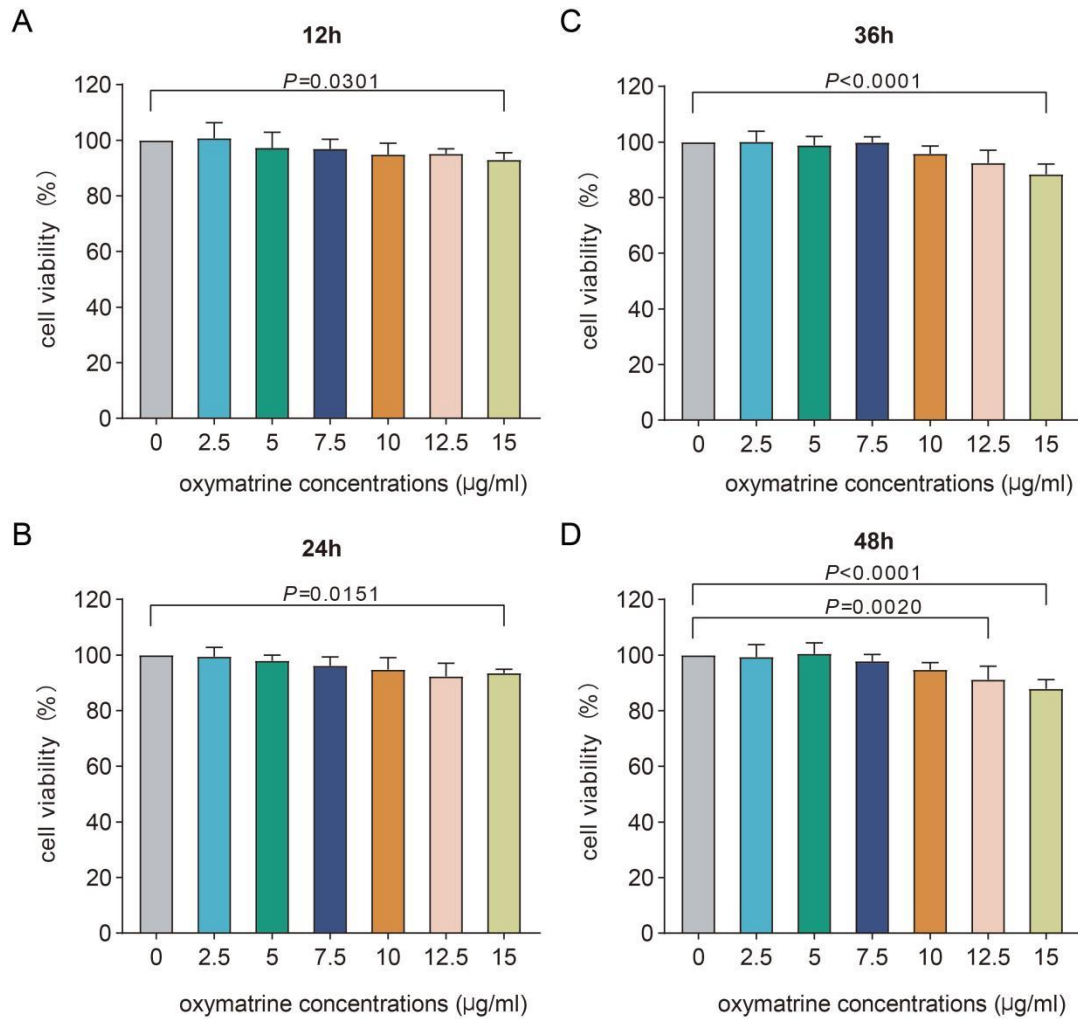


Figure S5. Cell Viability in PMVECs Following Exposure to a Narrow Concentration Range of OMT Over Various Time Intervals.

(A-D) This bar graph illustrates the impact of varying concentrations of Oxymatrine (OMT) on the viability of Pulmonary Microvascular Endothelial Cells (PMVECs) across four distinct time intervals: 12h (A), 24h (B), 36h (C), and 48h (D). The cell viability post-OMT exposure was quantitatively evaluated using the CCK-8 assay.

Experiments were performed in triplicate, and the mean \pm S.D. ($n = 3$) is shown. P values were determined by non-parametric one-way ANOVA.